Exchange interactions of spin-active metallofullerenes in solid-state carbon networks

Mujtaba Zaka,[1] Jamie H. Warner,[1,*] Yasuhiro Ito,[1] John J. L. Morton,[1] Mark H. Rümmeli,[2] Thomas Pichler,[3] Arzhang Ardavan,[4] Hisanori Shinohara,[5] and G. Andrew D. Briggs[1]

[1]*Department of Materials, Quantum Information Processing Interdisciplinary Research Collaboration, University of Oxford, Parks Rd., Oxford OX1 3PH, United Kingdom*

[2]*IFW Dresden, P.O. Box 270116, D-01171 Dresden, Germany*

[3]*Fakultät für Physik, Universität Wien, Strudlhofgasse 4, 1090 Wien, Austria*

[4]*Clarendon Laboratory, Department of Physics, Quantum Information Processing Interdisciplinary Research Collaboration, University of Oxford, Parks Rd., Oxford OX1 3PH, United Kingdom*

[5]*Department of Chemistry and Institute for Advanced Research, Nagoya University, Furo-Cho, Chikusa-ku, Nagoya 464-8602, Japan*

(Received 12 May 2009; revised manuscript received 4 January 2010; published 22 February 2010)

The electron paramagnetic resonance (EPR) of spin-active metallofullerenes (MFs) La@C_{82} and Sc@C_{82} diluted in solid-state C_{60} crystalline matrices with molar concentrations varying from 0.4% to 100% are investigated. For dilute concentrations, the hyperfine structure of the MFs is resolved, and as the concentration increases exchange narrowing is observed leading to a single peak in the EPR. Sc@C_{82} MFs are inserted into single-walled carbon nanotubes to form peapods with concentrations of 10% and 0.1%, diluted with C_{60}. For the case of peapods containing 10% Sc@C_{82} a strong narrow peak is observed in *X*-band CW EPR, but not pulsed measurements. Peapods containing Ce@C_{82} MFs are prepared and these also show similar CW EPR to the Sc@C_{82}, indicating the peak arises from charge transfer with the SWNT.

DOI: 10.1103/PhysRevB.81.075424 PACS number(s): 81.07.−b, 76.30.−v, 81.05.ub

I. INTRODUCTION

The successful utilization of carbon nanomaterials in future electron spin-based technologies is highly dependent upon the ability to control their assembly at the nanoscale to form tailored solid-state architectures. Fullerenes can hold single electron spins with long coherence times and, therefore, have promise as building blocks for electron spin based technologies.[1] Fullerenes can be inserted into the interior of single-walled carbon nanotubes (SWNTs) to form peapods,[2] offering a way to noncovalently produce highly ordered one-dimensional (1D) spin chains,[3,4] with possible applications in quantum information and nanoscale spintronics.[1,5] There remain many open questions regarding the nature of the spin and spin-spin interaction in such systems, which will be key to their future integration in devices. We wish to investigate the nature of the interactions between spins within the chain and how this is affected by the presence of the nanotube. Here, we address this by analyzing spin-spin interactions between metallofullerenes in both three dimensional (3D) (crystals) and 1D (peapods). Previous studies on pure macroscopic crystals have shown very broad EPR spectra resulting from strong interfullerene spin interactions,[6] or investigated the dilute spin limit in solution, where spin interactions are negligible.[7,8]

To explore the region between these limits, we dilute the spin-active fullerenes within a matrix of diamagnetic C_{60}. This permits the tuning of mean fullerene separation and thus interfullerene spin interactions. We demonstrate that exchange interactions between MFs occur in C_{60} crystals and can be controlled by varying the molar concentration of MFs in C_{60} from 0.8% to 100%. We then insert Sc@C_{82} into SWNTs to form peapods and examine the changes in the EPR spectrum. Recent studies on the spin dynamics of N@C_{60} peapods found charge transfer is minimal, consistent with the fact that N@C_{60} spin is well localized within the fullerene cage.[9,10]

II. EXPERIMENTAL

Metallofullerenes (MFs) of La@C_{82},[11] Sc@C_{82},[12,13] and Y@C_{82},[14] consisting of a fullerene cage and encapsulated metal atom, possess many unique properties due to the charge transfer from the metal atom to the fullerene cage.[15] Metallofullerenes M@C_{82} [M=La, Sc, Ce] were produced using arc-discharge method.[15] The MFs were purified by high performance liquid chromatography and characterized using MALDI-TOF mass spectroscopy.

SWNTs with narrow diameter distribution (1.4–1.6 nm) in the range suitable for filling with MFs can be produced using laser ablation with the nonmagnetic catalyst Pt/Rh/Re and are ideal for EPR studies of peapods.[16] Pt/Rh/Re SWNTs were produced using laser ablation[16] and purified by a previously reported procedure.[17]

MF doped C_{60} crystals were formed by slowly removing the solvent from a CS_2 solution of known C_{60}:MF concentration under vacuum. All samples for EPR were degassed and sealed in a quartz tube under vacuum. The number of MFs was kept constant and the amount of C_{60} varied to obtain different concentrations. Peapods were produced using a hot vapor phase filling method.[3] Fullerenes in a CS_2 solution were dropped onto a SWNT mat and the solvent was allowed to evaporate. The sample was then sealed in a quartz tube under vacuum and heated at 450 °C for 4 days to form peapods. EPR measurements were performed using a Bruker EMX spectrometer at 9.4 GHz in the 5–300 K temperature range using an Oxford ESR900 cryostat. High-resolution transmission electron microscopy (HRTEM) was performed on a JEOL 4000EX operating at 80 kV.

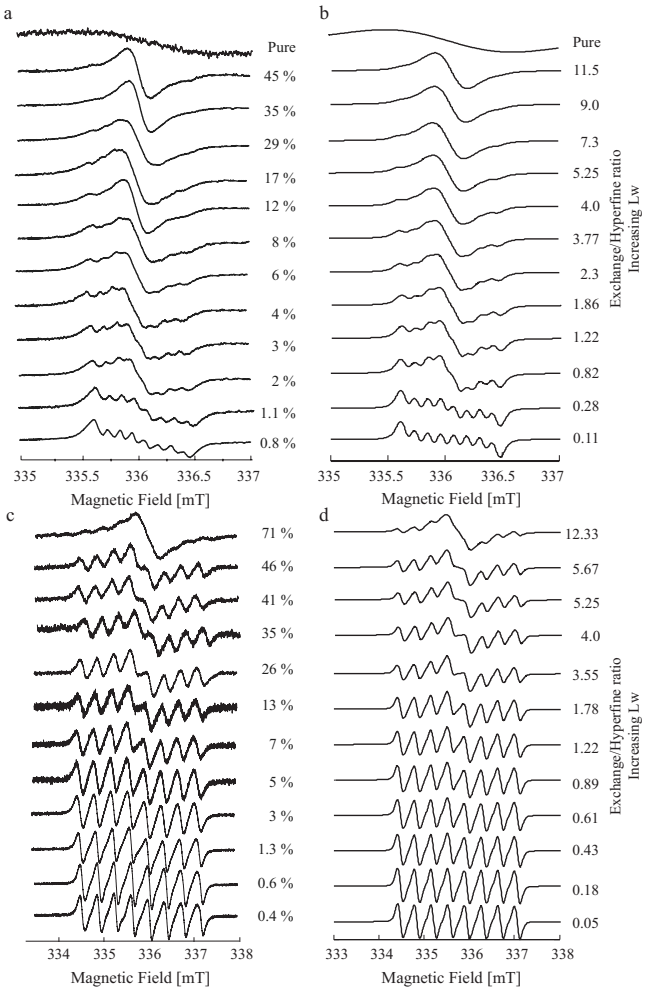

FIG. 1. (a) CW EPR of La@C_{82} with varying molar concentration in C_{60} crystals. (b) Model of La@C_{82} with increasing exchange/hyperfine ratio and increasing linewidth. (c) CW EPR of Sc@C_{82} with varying molar concentration in C_{60} crystals. (d) Model of Sc@C_{82} with increasing exchange/hyperfine ratio and increasing linewidth. Experimental parameters: field modulation 100 kHz, 1 G; microwave power 1.976 mW; temperature 300 K.

III. RESULTS

A. 3D MF Crystals

Figure 1(a) shows EPR spectra of La@C_{82} diluted in C_{60}, with a molar La@C_{82}:C_{60} concentration range of 0.8%–100%. At a low concentration of 0.8% hyperfine structure of the La@C_{82} is well resolved and as the concentration increases the hyperfine structure becomes broader and a single narrow peak emerges from the center. At concentrations over 20%, all of the hyperfine structure is lost and only the single peak remains. At a concentration of 100%, we found the EPR spectrum to consist of a single broad peak with linewidth of 12 G, in contrary to previous reports.[18] This may be due to a difference in purity of the La@C_{82}, which significantly influences the spectrum.

In order to understand the EPR spectra observed in Fig. 1(a), we simulated the EPR spectrum of La@C_{82} using the MATLAB *Easyspin* software.[19] Since exchange interactions are strongly dependent upon wave function overlap, exchange coupling will most likely only occur in clusters of MFs within the C_{60} crystal. Isolated MFs, surrounded by empty caged C_{60}, should show the hyperfine interaction between the nuclear (La or Sc) and electron spin of the MF. The ratio of clustered MFs to isolated MFs should increase with concentration of MF species within a C_{60} crystal. With increasing concentration of MFs we also expect the dipole-dipole interaction to increase due to a decrease in the average inter-MF separation, leading to broadening of the EPR signal, as shown in the pure case.

In our model we assume that any exchange coupling between MF clusters is a constant J, since the largest J value arises from MF nearest neighbors, therefore smaller couplings can be ignored. To account for the dipole-dipole interactions the linewidth is increased with concentration. We simulated two systems, a two-spin exchange-coupled system to represent MF clusters and a single spin hyperfine interaction system for isolated MFs. By combining different ratios of the exchange coupled and hyperfine interaction system, we can successfully reproduce the experimental results as shown in Fig. 1(b). The exchange interaction J coupling strength for the MF clusters is set to 13 MHz, and the linewidth for each component is shown in Table I. The ratios of exchange coupled MF clusters and hyperfine interaction were determined to match the experimental results for each concentration.

Similar experiments were performed on Sc@C_{82}, Fig. 1(c), for dilutions between 0.4% and 71% again using the same preparation methods and the same amount of Sc@C_{82} in each case to keep the total number of spins constant. The stronger hyperfine interaction in Sc@C_{82} than La@C_{82} makes it more robust against exchange narrowing and the hyperfine structure is retained up to a concentration of 46%.[20] A similar simulation model was used to effectively reproduce the concentration dependence of the Sc@C_{82} EPR spectrum and is presented in Fig. 1(d). The J coupling for the MF clusters is set to 60 MHz, and the linewidth for each component is shown in Table I. The stronger hyperfine of Sc@C_{82} makes it more robust against exchange narrowing; as demonstrated through the value of exchange coupling used in the simulation in Fig. 1(d) compared to that mentioned above for La@C_{82}.

B. 1D MF Peapods

A recent report suggested that the interaction of La@C_{82} with SWNTs prepared using the supergrowth method resulted in the loss of the hyperfine structure in the EPR,[18] attributed to charge transfer between the La@C_{82} and SWNTs. We investigate this further using Sc@C_{82} where the (undisturbed) hyperfine interaction is larger.[21] Peapods of Sc@C_{82} produce a highly ordered 1D array of spins and may show different spin-spin interactions compared to 3D crystals. Visual indication of the filling and purity of Sc@C_{82} peapods was achieved by performing HRTEM. Raw SWNTs contain high levels of amorphous and graphitic carbon as well as catalyst particles as shown in Figs. 2(a) and 2(b), which can affect the EPR spectra. Removal of carbon

TABLE I. Line width parameters used in the simulation relating to produce the simulated spectra in Figs. 1(b) and 1(d), for La@C_{82} and Sc@C_{82}, respectively.

La@C_{82}				Sc@C_{82}			
MF Molar Content (%)	Ratio Exchange/Hyperfine	Hyperfine (LW/mT)	Exchange (LW/mT)	MF Molar Content (%)	Ratio Exchange/Hyperfine	Hyperfine (LW/mT)	Exchange (LW/mT)
Pure	Pure	0.801	1.221	71	12.33	0.139	0.406
45	11.50	0.105	0.183	46	5.67	0.136	0.376
35	9.00	0.102	0.178	41	5.25	0.136	0.368
29	7.33	0.099	0.175	35	4.00	0.135	0.358
17	5.25	0.093	0.166	26	3.55	0.133	0.339
12	4.00	0.089	0.160	13	1.78	0.130	0.299
8	3.17	0.085	0.153	7	1.22	0.126	0.268
6	2.70	0.082	0.149	5	0.89	0.125	0.252
4	2.03	0.078	0.143	3	0.61	0.122	0.230
3	1.50	0.076	0.139	1.3	0.43	0.118	0.198
2	1.22	0.072	0.134	0.6	0.18	0.115	0.172
1.1	0.28	0.067	0.126	0.4	0.05	0.113	0.160
0.8	0.11	0.064	0.122				

impurities and catalyst particles produced purified SWNTs, shown in Figs. 2(c) and 2(d). TEM studies of the 10% Sc@C_{82}:C_{60} peapod sample shown in Fig. 2(e) indicate a high level of filling of SWNTs up to approximately 60%–80%, with reduced amounts of amorphous carbon and catalyst particles. Figure 2(f) shows a HRTEM image of a typical isolated peapod filled with fullerenes.

We measured the CW EPR spectrum with the fullerenes first on the outside of the SWNTs and then inside the SWNTs. These two measurements allow any change in the interactions caused by one-dimensional filling inside of the nanotube to be identified. We prepared peapods with a molar concentration of 10% and 0.1% Sc@C_{82}. Figure 3(a) shows the CW EPR spectra of the 10% Sc@C_{82}:C_{60} sample on the outside of the SWNTs, with 8 peaks attributed to the hyperfine structure of Sc@C_{82} resolved. The 0.1% Sc@C_{82} sample, Fig. 3(b), shows almost no noticeable structure due to the minimal amount of Sc@C_{82} and the substantial amount of EPR silent C_{60}.

Figure 3(c) shows that upon encapsulation of the 10% Sc@C_{82}:C_{60} peapods the hyperfine structure disappears. The spectrum contains a narrow peak with linewidth ~1 G and a broader background peak of linewidth 4.5 G. This broad background peak is also present in the diluted 0.1% Sc@C_{82} peapod sample, shown in Fig. 3(d), suggesting it should not be attributed to the metallofullerenes, but arises instead from some other source such as, amorphous carbon or a catalyst carbon. The narrow 1 G peak has two possible origins, charge transfer between the nanotube and Sc@C_{82} resulting in a spin $\frac{1}{2}$ electron or hole on the SWNT with no measurable Sc hyperfine interaction, or the presence of

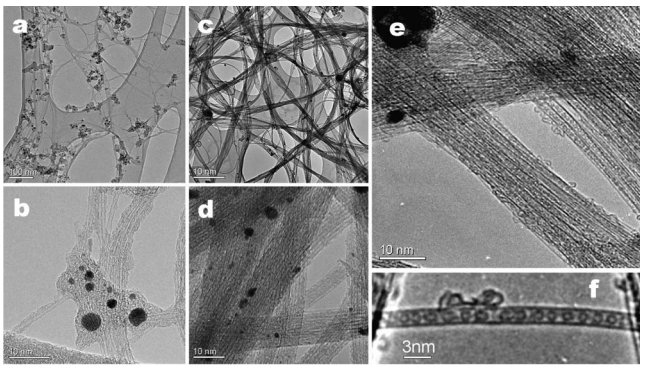

FIG. 2. (a) TEM image of raw SWNT bundles. (b) TEM image of raw SWNTs with higher magnification. (c) TEM image of purified SWNTs. (d) TEM of purified SWNTs with higher magnification. (e) TEM image of Sc@C_{82}:C_{60} peapods. (f) TEM image of isolated Sc@C_{82}:C_{60} peapods with higher magnification.

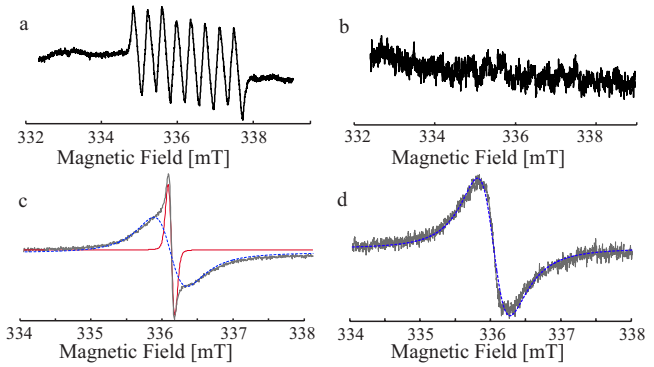

FIG. 3. (Color online) (a) CW EPR of 10% Sc@C_{82}:C_{60} upon the surface of the SWNT. (b) CW EPR of 0.1% Sc@C_{82}:C_{60} upon the surface of the SWNT. (c) CW EPR of 10% Sc@C_{82}:C_{60} peapods, including a model of the two components, the narrow and broad peak. (d) CW EPR of 0.1% Sc@C_{82}:C_{60} peapods, with an overlay of a model of the broad feature. Experimental parameters: field modulation 100 kHz, 1 G; microwave power 1.973 mW; temperature 300 K.

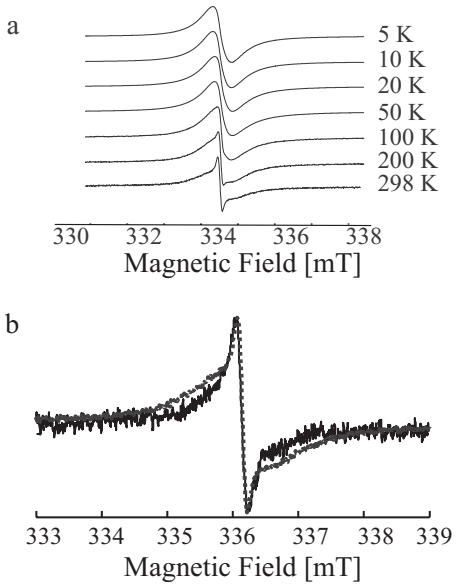

FIG. 4. (a) (i) Low temperature EPR measurement of 10% Sc@C_{82}:C_{60} peapods, indicating the change in intensity of the signal with temperature, where the spectrum has been normalized. (b) C.W EPR of Ce@C_{82} peapods (black) and Sc@C_{82}:C_{60} peapods (dotted) showing a narrow and broad feature.

strong MF exchange interactions that causes narrowing.

To elucidate which of these two possible mechanisms could be responsible for the narrow peak further dynamics of Sc@C_{82}:C_{60} peapods were studied. Temperature dependence of CW EPR was examined between 5 and 298 K and is presented in Fig. 4(a)(i). The spectra have been normalized, as the intensity of the peaks increased at lower temperatures. Figure 4(a)(i) shows that at as the temperature decreases the broad component dominates. The inability to resolve the narrow peak associated with the metallofullerenes makes it difficult to extract valuable information from the temperature-dependent study in Fig. 4(a). Using pulsed EPR, we conducted field-dependent Hahn echo (τ =240 ns) measurements from the 10% Sc@C_{82} peapod and observed only a contribution from the broad background signal. The narrow peak showed no contribution to the Hahn echo, indicating it is being narrowed through spin-spin exchange coupling or spin delocalization (such that $T_2=T_2^*$). Electron spin echo envelope modulation measurements also showed no signs of coupling to Sc nuclear spins. The inability to probe the EPR signal attributed to the metallofullerenes in SWNT peapods using pulsed EPR techniques prompted an alternative approach for determining the underlying nature of the spin signal.

Ce@C_{82} MFs have similar charge transfer from the metal atom to the cage with 3 valence electrons donated to the C_{82} cage, but Ce@C_{82} does not exhibit measurable room temperature EPR signals.[22] Ce@C_{82}, therefore, provides a convenient comparison for the spin active Sc@$_{82}$. We filled SWNTs with Ce@C_{82} to produce peapods and measured the room temperature CW EPR spectrum, shown in Fig. 4(b). The EPR spectrum of the Ce@C_{82} peapods in Fig. 4(b) has been overlaid with the EPR spectrum for Sc@C_{82} peapods; in both cases a narrow 1 G peak and a broad background peak are present. This provides strong evidence that the narrow peak arises from charge transfer between the SWNT and MFs and not from exchange narrowing between MFs. This charge transfer results in a delocalized spin on the SWNT that has no measurable hyperfine interaction with the metal nuclear spin. The unpaired electron remaining on the Ce atom is in a 4*f* orbital, with large angular momentum and spin-obit coupling.[22] This results in the broadening of any EPR signal and explains why it is not observed in our measurements. These results show that when MFs are inserted into SWNTs the spin dynamics change significantly with interactions between the MFs and SWNT host.

In summary, we have shown how the environment can influence the spin dynamics of La@C_{82} and Sc@C_{82} and lead to exchange interactions and charge transfer. Inserting spin-active MFs into SWNTs to form peapods resulted in the loss of measurable hyperfine structure attributed to charge-transfer interactions with the SWNTs. These results provide important information needed for the further advancement of solid-state architectures for spin-dependent transport studies and devices using spin-active metallofullerenes.

ACKNOWLEDGMENTS

This research is part of QIPIRC (www.qipirc.org) funded by EPSRC (Grant No. GR/S82176/01). J.H.W. thanks the Sasakawa fund for support. J.H.W. is supported by the Glasstone Fund and Brasenose College, Oxford. H.S. is supported by the JSPS-CREST Program on Nanocarbons. J.J.L.M is supported by St. Johns College, Oxford and by the Royal Society. T.P and M.R are supported by DFG under Grant No. PI440/3/4/5.

*jamie.warner@materials.ox.ac.uk

[1] S. C. Benjamin, A. Ardavan, G. A. D. Briggs, D. A. Britz, D. Gunlycke, J. Jefferson, M. A. G. Jones, D. F. Leigh, B. W. Lovett, A. N. Khlobystov, S. A. Lyon, J. Morton, K. Porfyrakis, M. R. Sambrook, and A. M. Tyryshkin, J. Phys.: Condens. Matter **18**, S867 (2006).

[2] B. W. Smith, M. Monthioux, and D. E. Luzzi, Nature (London) **396**, 323 (1998).

[3] J. H. Warner, A. A. R. Watt, L. Ge, K. Porfyrakis, T. Akachi, H. Okimoto, Y. Ito, A. Ardavan, B. Montanari, J. H. Jefferson, N. M. Harrison, H. Shinohara, and G. A. D. Briggs, Nano Lett. **8**, 1005 (2008).

[4] L. Ge, B. Montanari, J. H. Jefferson, D. G. Pettifor, N. M. Harrison, and G. A. D. Briggs, Phys. Rev. B **77**, 235416 (2008).

[5] I. Zutić, J. Fabian, and S. Das Sarma, Rev. Mod. Phys. **76**, 323 (2004).

[6] C. J. Nuttall, Y. Inada, K. Nagai, and Y. Iwasa, Phys. Rev. B **62**, 8592 (2000).

[7] N. Weiden, T. Kato, and K.-P. Dinse, J. Phys. Chem. B **108**, 9469 (2004).
[8] S. Knorr, A. Grupp, M. Mehring, U. Kirbach, A. Bartl, and L. Dunsch, Appl. Phys. A: Mater. Sci. Process. **66**, 257 (1998).
[9] C. Knapp, K.-P. Dinse, B. Pietzak, M. Waiblinger, and A. Weidinger, Chem. Phys. Lett. **272**, 433 (1997).
[10] A. Weidinger, M. Waiblinger, B. Pietzak, and T. A. Murphy, Appl. Phys. A: Mater. Sci. Process. **66**, 287 (1998).
[11] Y. Chai, T. Cuo, C. Jin, R. E. Haufler, L. P. F. Chibante, J. Fure, L. Wang, J. M. Alford, and R. E. Smalley, J. Phys. Chem. **95**, 7564 (1991).
[12] H. Shinohara, H. Sato, M. Ohkohchi, Y. Ando, T. Kodama, T. Shida, T. Kato, and Y. Saito, Nature (London) **357**, 52 (1992).
[13] C. S. Yannoni, M. Hoinkis, M. S. de Vries, D. S. Bethune, J. R. Salem, M. S. Crowder, and R. D. Johnson, Science **256**, 1191 (1992).
[14] K. Kikuchi, Y. Nakao, S. Suzuki, and Y. Achiba, J. Am. Chem. Soc. **116**, 9367 (1994).
[15] H. Shinohara, Rep. Prog. Phys. **63**, 843 (2000).
[16] M. H. Rümmeli, C. Kramberger, M. Löffler, O. Jost, M. Bystrzejewski, A. Grüneis, T. Gemming, W. Pompe, B. Büchner, and T. Pichler, J. Phys. Chem. C **111**, 4094 (2007).
[17] R. Schönfelder, M. H. Rümmeli, W. Gruner, M. Löffler, J. Acker, V. Hoffmann, T. Gemming, B. Büchner, and T. Pichler, Nanotechnology **18**, 375601 (2007).
[18] P. Jakes, A. Gembus, K.-P. Dinse, and K. Hata, J. Chem. Phys. **128**, 052306 (2008).
[19] S. Stoll and A. Schweiger, J. Magn. Reson. **178**, 42 (2006).
[20] G. W. Morley, B. J. Herbert, S. M. Lee, K. Porfyrakis, T. J. S. Dennis, D. Nguyen-Manh, R. Scipioni, J. van Tol, A. P. Horsfield, A. Ardavan, D. G. Pettifor, J. C. Green, and G. A. D. Briggs, Nanotechnology **16**, 2469 (2005).
[21] Y. Ito, W. Fujita, T. Okazaki, T. Sugai, K. Awaga, E. Nishibori, M. Takata, M. Sakata, and H. Shinohara, ChemPhysChem **8**, 1019 (2007).
[22] T. Wakahara, J. Kobayashi, M. Yamada, Y. Maeda, T. Tsuchiya, M. Okamura, T. Akasaka, M. Waelchli, K. Kobayashi, S. Nagase, T. Kato, M. Kako, K. Yamamoto, and K. M. Kadish, J. Am. Chem. Soc. **126**, 4883 (2004).